Interaction of Al-induced peptide backbone ring structure with the sidechains of His, Phe, Trp and Tyr[*]

WU Qing-Lei (吴清雷)[1,2] and SONG Bo (宋波)[1,†]

[1]*Division of Interfacial Water and Laboratory of Physical Biology,*
Key Laboratory of Interfacial Physics and Technology, Shanghai Institute of Applied Physics,
Chinese Academy of Sciences, Shanghai 201800, China
[2]*University of Chinese Academy of Sciences, Beijing 100049, China*

Aluminium is widely used as an antimicrobial coagulant, food additive, and cookware. However, many reports indicate that aluminium may be a critical factor in many amyloid diseases, such as Alzheimer's disease and Parkinson's disease. Unfortunately, the underlying mechanism is still poorly understood, which limits efforts to prevent and treat these diseases. In this paper, using an ab initio method, we studied the interaction of Al-backbone ring structure with the π-electron-rich sidechains of His, Phe, Trp, and Tyr. We found that in the absence of water, the Al-backbone ring can stably bind with those sidechains. In the presence of water, the Al-backbone ring can bind to the His sidechain and cannot bind to the other sidechains. As revealed by further investigations, this could be attributed to the fact that there was a coordinate bond of the Al-backbone ring with the His sidechain, while there were the π-π stacking and cation-π-like interactions with the other sidechains. These findings potentially provide a molecular understanding of Al-related toxicity, and may be helpful in designing drugs for those aforementioned aluminum-linked diseases and encourage treatment of Al-polluted water.

Keywords: Ring structure, Al-backbone, Sidechain, Interaction

I. INTRODUCTION

Extensive evidences have shown that aluminum ions were a potent neurotoxicant, both in experimental animals and in humans [1–4]. It has lead to an increased interest in Al in antimicrobial coagulants [5–8], food additives, and cookware [9–11]. The first studies demonstrating Al neurotoxicity in experimental animals were conducted by Siem and Döllken more than 100 years ago [12]. In 1965, it was shown that intracerebral inoculation of Al phosphate in rabbits resulted in neurofibrillary degeneration of 'striking resemblance' to the neurofibrillary tangles of Alzheimer's disease (AD) [13, 14], thereby initiating the contentious debate of the role of Al in AD. In 1973, the increased concentrations of Al were found in the brains of patients with AD [15]. In 1985, Perl and his coworkers studied the relationship of aluminum to Alzheimer's disease, and identified abnormal accumulations of aluminum within neurons derived from Alzheimer's disease patients containing neurofibrillary tangles [16]. In 2001, Trond and his colleagues reported the epidemiological evidence linking Al and AD [17]. With the study of biomolecules, the close relationship between aluminum and health, along with its mechanisms, has become interesting [18–21]. Recently, it was reported that Al ions can induce the formation of backbone ring structures in peptides, largely destabilizing the proteins and resulting in irreversible denaturation [22], which provides a new way to understand Al-related toxicity.

Non-covalent interaction is crucial in a variety of phenomena in biology [23–25]. The interaction among molecules not bound by chemical bonds made possible the formation of supramolecular units, which form the basis of many aspects of supramolecular chemistry and nanotechnology [26]. In biological systems, non-covalent interactions were responsible for phenomena such as molecular recognition [27] and played a crucial role in enzymatic catalysis [28], protein folding [29, 30], and even process, such as ion transport of recognition [31–33]. In recent years, studies of model systems and analysis of biological macromolecular structures have established the importance of the cation-π interaction as a force for molecular recognition [34]. In the absence of water, the binding of simple cations to benzene and related structures was shown to be quite substantial, comparable even to cation-water interactions [35]. Through the sidechains of aromatic amino acids, novel binding sites for cationic ligands can be constructed [36]. Meanwhile, the usual π-π interaction was an offset or slipped stacking, i.e., the rings were parallelly displaced. Such a parallelly-displaced structure results from the contribution of π electron attraction [37, 38]. It was shown that π-π interactions were not due to an electrostatic attraction between the two π-systems, but occurred when the attractive interactions outweighed the contributions of π-electron repulsion [39, 40]. It should be noted that all the above non-covalent interactions are based on π-electron-rich molecular structures.

In this paper, we explore the interactions between the Al-induced backbone ring structure and the π-electron-rich sidechains of His, Phe, Trp, and Tyr. It is observed that the Al-induced complex is able to stably bind to these sidechains in

---

[†] Corresponding author, bosong@sinap.ac.cn

the absence of water molecules. Meanwhile, the Al-backbone ring can bind to the His sidechain and can not bind to the other sidechains in the presence of water molecules. The water-independent adsorption can be attributed to the coordinate bond between the Al ion of the backbone-ring structure and the N atom of His sidechain. The mechanism of water-dependent adsorption is then revealed to be the following. The Al-induced backbone ring structure first induced a redistribution of the π electrons when it is close to the ring layers of the Phe, Trp, and Tyr sidechains. After that, an attraction like cation-π and π-π stacking interaction occures between the Al-induced complex and the sidechain layers, which depends on the presence of water molecules. These findings have the potential to lead to an understanding of the effect of Al-backbone ring structure on the sidechains of amino acids, and even the pathogenic mechanisms of amyloid diseases.

II. METHODS

All of our calculations were performed by the second-order Mϕller-Plesset perturbation theory (MP2), as implemented in the Gaussian09 package with the 6-31+G(d,p) basis set of triple-zeta quality and including diffuse functions applied on all atoms, which has been widely used to study the interaction between Al-induced backbone ring structure and π-electron-rich amino acids. Once a stationary point has been reached, a frequency analysis was carried out to ensure that the structure corresponded to a minimum in the potential energy surface of the complex.
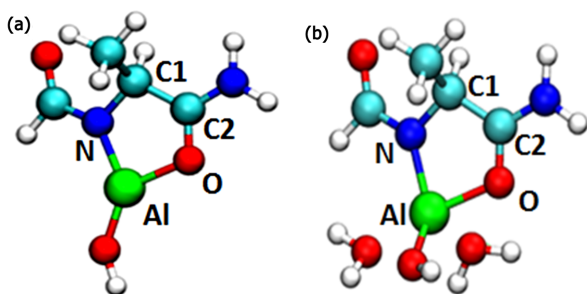

Fig. 1. (Color online) Al-induced backbone-ring structure. The cyan, blue, red, white, and green balls represent carbon, nitrogen, oxygen, hydrogen, and aluminum, respectively. (a) The Al-backbone complex consists of [AlOH]$^{2+}$ and a model peptide, HCO-Ala-NH$_2$, where Al ions bind on the peptide backbone by forming a ring structures, and the hydrogen atom initially attached to the amide nitrogen N is substituted by the Al ion. (b) The corresponding Al-backbone ring complex with H$_2$O molecules is formed by [AlOH $\cdot$ (H$_2$O)$_4$]$^{2+}$ [41] and the peptide, HCO-Ala-NH$_2$. The hydrated Al ion interacts with the O atom on the peptide backbone first and one H$_2$O molecule is released. Then it forms the ring structure by further interacting with the N atom and neighboring O atom on the peptide backbone with another H$_2$O molecule dropped.

III. RESULTS AND DISCUSSION

To study the interaction of the Al-induced backbone ring structure [22] with residue sidechains, we first applied an Al-backbone ring structure in the absence of water molecules, formed by [AlOH]$^{2+}$ and a model peptide, HCO-Ala-NH$_2$ (Fig. 1(a)). The hydrogen atom initially attached to the amide nitrogen N was substituted by the Al ion, and the Al ions simultaneously chemically bound to the amide nitrogen N and carboxyl oxygen O on the backbone. Therefore, the backbone structure consisted of the Al ion together with the α carbon, C1, carbonyl carbon, C2, amide nitrogen, N, and carboxyl oxygen, O, atoms. We simulated the binding of the Al-backbone ring structure with the sidechains of His, Phe, Trp, and Tyr. The relaxed structures are presented in Fig. 2. The dihedral angle (Table 1) between the ring and His sidechain was 90°, while the dihedral angles between the ring and sidechain planes of Phe, Trp, and Tyr were 48°, 43°, and 37°, respectively. Therefore, the Phe, Trp, and Tyr sidechains almost stacked over the backbone ring structure, which was clearly different from the His sidechain. We further calculated the binding energy of the ring structure with the sidechains by the formula,

$$\begin{aligned} E_{\text{binding}} = &E(\text{all complex including no water molecule}) \\ &- E(\text{the ring structure with no water molecule}) \\ &- E(\text{sidechain}), \end{aligned}$$
(1)

where E_{binding} denotes the binding energy of the backbone ring and sidechain, while the first, second, and third term in the right side of equation indicate the energies of the complex formed by the Al-backbone ring structure and the sidechains, the Al-backbone ring structure and the sidechain of the amino acid. We have calculated a series of binding energies and carried out frequency analysis of different displacements of the His, Phe, Trp, and Tyr to ensure that the structure we have selected corresponds to a minimum in the potential energy surface of the complex. The results are shown in Table 1. For the interaction of the Al-backbone ring with His sidechain, the binding energy reached -2.91 eV, which means that the binding is very stable in absence of water. This can be attributed to the coordinate bond of the Al ion with the N atom of His sidechain [42, 43]. Namely, N atom of the histidine tends to grasp the Al ion through a coordinate bond as the electron-pair-donor. The coordinate bond forms when the electrons of the N atom from the histidine residue are shared between N and Al atoms. In the case of Phe, Trp, and Tyr sidechains, the binding energies of the backbone ring were -1.63, -2.10 and -1.69 eV, respectively, which indicates that the binding between the backbone ring and these sidechains are also stable in absence of water. These binding energies were clearly weaker than the binding energy between the backbone ring and His sidechain, denoting the interactions of the backbone ring with the Phe, Trp, and Tyr sidechains are weaker than that with the His sidechain.

We also investigated the impact of water on the above binding by considering the first solvation shell of the Al aqua ion
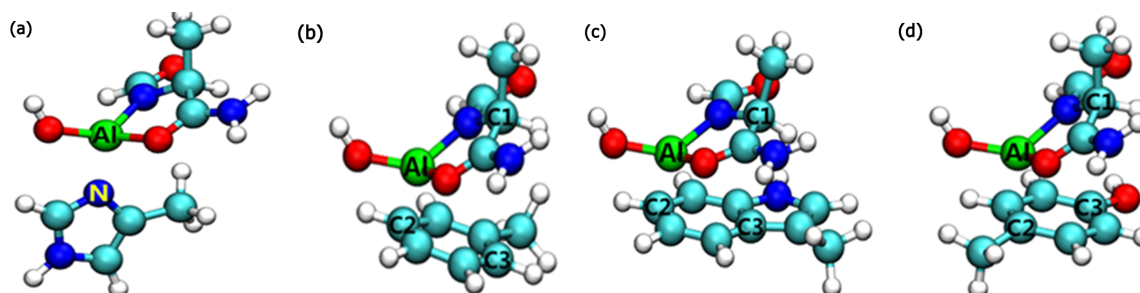
Fig. 2. (Color online) Interactions of Al-backbone ring with the sidechains of His (a), Phe (b), Trp (c), and Tyr (d). The cyan, blue, red, white and green balls represent carbon, nitrogen, oxygen, hydrogen, and aluminum, respectively. Figure (b)–(d) show a new type of stacking structure, which has a certain inclination compared to the π-π stacking. Figure (a) shows a strong coordination interaction, different from the stacking structure. In order to demonstrate the interaction clearly, we only retained the α carton. The backbone of the four amino acid is replaced by the hydrogen atom.
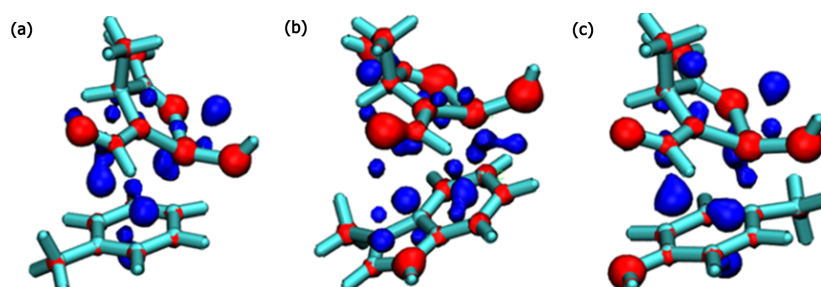

Fig. 3. (Color online) Redistribution of electronic density in Al-backbone ring and sidechains. The blue cloud denotes the electron-density change $\Delta D > 0$ (regions accepting electrons), and the red cloud with the isosurface indicates $\Delta D < 0$ (regions losing electrons). Here, the Al-backbone conformation with its ring structure close to the π layer on the sidechains is presented as an example. (a) Phe, (b) Trp and (c) Tyr.

TABLE 1. Dihedral angles and binding energies of Al-backbone ring with residue sidechains

	His	Phe	Trp	Tyr
Dihedral angles (°)	90	48	43	37
Binding energy[a] (eV)	−2.91	−1.63	−2.10	−1.69
Binding energy[b] (eV)	−1.06	0.35	−0.11	0.24

[a] absence of water molecules.
[b] presence of water molecules.

$([AlOH(H_2O)_4]^{2+})$. The binding energy in the presence of the first water shell was calculated by the formula as follows,

$$
\begin{aligned}
E_{\text{binding}} =\, & E(\text{all complex including two water molecules}) \\
& + E(\text{H}_2\text{O}) \\
& - E(\text{the ring structure pulse two water molecules}) \\
& - E(\text{sidechain}),
\end{aligned}
\tag{2}
$$

where E_{binding} denotes the binding energy of the backbone ring and sidechain in the presence of water molecules, while the first, second, third, and fourth terms in the right side of equation denote the energies of the complex composed by the Al-backbone ring structure and the residue sidechain with one water molecule attached to the Al ion, one water molecule which drops off when the complex forms, the Al-backbone ring with two water molecules tied to the Al ion, and the residue sidechain. As presented by the results in Table 1, when introducing water molecules, the binding energies were reduced to $-1.06\,\text{eV}$ for the His sidechain, $0.35\,\text{eV}$ for the Phe sidechain, $-0.11\,\text{eV}$ for the Trp sidechain, and $0.24\,\text{eV}$ for the Tyr sidechain, respectively. This indicates that in the presence of water, the binding strength of backbone ring structure with these sidechains can be significantly reduced, especially the binding of Phe, Trp and Tyr sidechains, which become unstable. It is noted that the stable binding of the Al-backbone ring with the His sidechain in the presence of water molecules can be attributed to the coordinate bond between the Al ion and the N atom of His.

To reveal the physics underlying the water-dependent binding between the Al-backbone ring structure and the sidechains of Phe, Trp, and Tyr, we further calculated the redistribution of the electron density when the Al-backbone ring was bound to the sidechain by the formula,

$$
\begin{aligned}
\Delta D =\, & D(\text{BackboneRing + sidechain}) \\
& - D(\text{BackboneRing}) - D(\text{sidechain}),
\end{aligned}
\tag{3}
$$

where the first, second, and third terms on the right side of equation represents the electron density of the complex, the Al-backbone ring structure, and the sidechain, respectively.
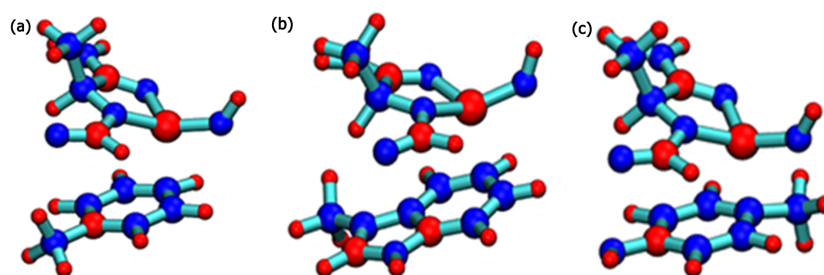
Fig. 4. (Color online) Distribution of positive and negative charges. The red and blue balls represent the atoms with positive and negative charges, respectively. (a) Phe, (b) Trp, and (c) Tyr.

The results are shown in Fig. 3. Blue clouds were clearly observed between the Al-backbone ring and the sidechains of Phe, Trp, and Tyr, which means that there are electrons shared between the backbone ring and sidechain, and, thus, π-π stacking interaction occurs between them. The π-π stacking interaction of two benzenes is about $-0.3\,\text{eV}$ [44], which is obviously weaker than the binding of the backbone ring with the sidechain. Therefore, besides π-π stacking, there should be other physics underlying these interactions. We further analyzed the atomic charges of the complex. As presented in Fig. 4, the positively charged Al ions were always close to the negatively charged atoms of sidechain, which indicates that there exists electrostatic attraction between the Al-backbone ring and the sidechains of Phe, Trp, and Tyr. Therefore, the Al ions in the backbone ring structure induce the re-arrangement of charges in the sidechain, resulting in a cation-π-like interaction between them [34–36, 45]. This will significantly increase the binding strength of the ring with those sidechains in the absence of water, which could be largely reduced by water molecules.

IV. CONCLUSION

We studied the interaction between the Al-backbone ring structure and the sidechains of His, Phe, Trp, and Tyr. It was found that in the absence of water, the Al-backbone ring can stably bind with those sidechains. In the presence of water, it can bind to the His sidechain, but cannot bind to the other sidechains. As revealed by further investigation, the underlying mechanism was the coordinate bond of the Al-backbone ring with the His sidechain, while there were the π-π stacking and cation-π-like interactions with the other sidechains. These findings are expected to help understand the effect of Al-backbone ring structure on the sidechains of amino acids, and even the pathogenic mechanism of Alzheimer's disease.

[1] Farrah S R, Goyal S M, Gerba C P, *et al*. Concentration of poliovirus from tap water onto membrane filters with aluminum chloride at ambient pH levels. Appl Environ Microb, 1978, **35**: 624–626.

[2] Lance J C and Gerba C P. Effect of ionic composition of suspending solution on virus adsorption by a soil column. Appl Environ Microb, 1984, **47**: 484–488.

[3] Driscoll C T, Baker J P, Bisogni J J, *et al*. Effect of aluminum speciation on fish in dilute acidified waters. Nature, 1980, **284**: 161–164. DOI: 10.1038/284161a0

[4] Crapper D R, Krishnan S S and Dalton A J. Brain aluminum distribution in Alzheimer's disease and experimental neurofibrillary degeneration. Science, 1973, **180**: 511–513. DOI: 10.1126/science.180.4085.511

[5] Hallett J P and Welton T. Room-temperature ionic liquids: solvents for synthesis and catalysis. Chem Rev, 2011, **111**: 3508–3576. DOI: 10.1021/cr1003248

[6] Gilbert R G, Gerba C P, Rice R C, *et al*. Virus and bacteria removal from wastewater by land treatment. Appl Environ Microb, 1976, **32**: 333–338.

[7] Banks W A and Kastin A J. Aluminum-induced neurotoxicity: alterations in membrane function at the blood-brain barrier.

Neurosci Biobehav R, 1989, **13**: 47–53. DOI: 10.1016/S0149-7634(89)80051-X

[8] Monath T P, Fowler E, Johnson C T, *et al*. An inactivated cell-culture vaccine against yellow fever. New Engl J Med, 2011, **364**: 1326–1333. DOI: 10.1056/NEJMoa1009303

[9] Marichai T, Ohata K, Bedoret D, *et al*. DNA released from dying host cells mediates aluminum adjuvant activity. Nat Med, 2011, **17**: 996–1002. DOI: 10.1038/nm.2403

[10] Cronan C S and Grigal D F. Use of calcium/aluminum ratios as indicators of stress in forest ecosystems. J Environ Qual, 1995, **24**: 209–226. DOI: 10.2134/jeq1995.00472425002400020002x

[11] Bolognin S, Messori L and Zatta P. Metal ion physiopathology in neurodegenerative disorders. Neuromol Med, 2009, **11**, 223–238. DOI: 10.1007/s12017-009-8102-1

[12] Alfrey A C. Aluminum and renal disease. Adv Clin Chem, 1983, **23**: 69–91. DOI: 10.1016/S0065-2423(08)60398-4

[13] Klatzo I, Wisniews H and Streiche E. Experimental production of neurofibrillary degeneration. 1. Light microscopic observations. J Neuropath Exp Neur, 1965, **24**: 187–199.

[14] Terry R D and Pena C. Experimental production of neurofibrillary degeneration. 2. Electron microscopy, phosphatase histo-

ChinaXiv

INTERACTION OF AL-INDUCED PEPTIDE . . .   Nucl. Sci. Tech. **26**, 040504 (2015)

chinaXiv:202306.00252v1

chemistry and electron probe analysis. J Neuropath Exp Neur, 1965, **24**: 200–210.

[15] Crapper D R, Krishnan S S and Dalton A J. Brain aluminum distribution in Alzheimer's disease and experimental neurofibrillary degeneration. Science, 1973, **180**: 511–513. DOI: 10.1126/science.180.4085.511

[16] Perl D P. Relationship of aluminum to Alzheimer's disease. Environ Health Persp, 1985, **63**: 149–153.

[17] Taniyasu Y, Kasu M and Makimoto T. An aluminum nitride light-emitting diode with a wavelength of 210 nanometres. Nature, 2006, **441**: 255–384. DOI: 10.1038/nature04760

[18] Gupta V K, Gupta M and Sharma S. Process development for the removal of lead and chromium from aqueous solutions using red mud–an aluminium industry waste. Wat Res, 2001, **35**: 1125–1134. DOI: 10.1016/S0043-1354(00)00389-4

[19] Tomljenovic L. Aluminum and Alzheimer's disease: after a century of controversy, is there a plausible link? J Alzheimers Dis, 2011, **23**: 567–598. DOI: 10.3233/JAD-2010-101494

[20] Shcherbatykh I and Carpenter D O. The role of metals in the etiology of Alzheimer's disease. J Alzheimers Dis, 2007, **11**: 191–205.

[21] Flaten T P. Aluminum as a risk factor in Alzheimer's disease, with emphasis on drinking water. Brain Res Bull, 2001, **55**: 187–196. DOI: 10.1016/S0361-9230(01)00459-2

[22] Song B, Sun Q, Li H K, *et al*. Irreversible denaturation of proteins through aluminum-induced formation of backbone ring structures. Angew Chem Int Ed., 2014, **53**: 6358–6363. DOI: 10.1002/ange.201307955

[23] Duan M Y, Song B, Shi G S, *et al*. Cation⊗3π: Cooperative interaction of a cation and three benzenes with an anomalous order in binding energy. J Am Chem Soc, 2012, **134**: 12104–12109. DOI: 10.1021/ja302918t

[24] Yang L, Sheng N, Tu Y S, *et al*. Friction force effects on vertical manipulation of nanoparticles. Nucl Sci Tech, 2012, **23**: 176–180.

[25] Shao S J, Guo P, Zhao L, *et al*. Ordered water monolayer on ionic model substrates studied by molecular dynamics simulations. Nucl Sci Tech, 2014, **25**: 020502. DOI: 10.13538/j.1001-8042/nst.25.020502

[26] Fields S and Song O K. A novel genetic system to detect protein–protein interactions. Nature, 1989, **340**: 245–246. DOI: 10.1038/340245a0

[27] Salonen L M, Ellermann M and Diederich F. Aromatic rings in chemical and biological recognition: energetics and structures. Angew Chem Int Edit, 2011, **50**: 4808–4842. DOI: 10.1002/anie.201007560

[28] Ueno T, Koshiyama T, Ohashi M, *et al*. Coordinated design of cofactor and active site structures in development of new protein catalysts. J Am Chem Soc, 2005, **127**: 6556–6562. DOI: 10.1021/ja045995q

[29] Matthews C R. Pathways of protein folding. Annu Rev Biochem, 1993, **62**: 653–683. DOI: 10.1146/annurev.bi.62.070193.003253

[30] Zechel D L and Withers S G. Glycosidase mechanisms: anatomy of a finely tuned catalyst. Accounts Chem Res, 2000, **33**: 11–18. DOI: 10.1002/chin.200015237

[31] Ionescu A R, Berces A, Zgierski M Z, *et al*. Conformational pathways of saturated six-membered rings. A static and dynamical density functional study. J Phys Chem A, 2005, **109**: 8096–8105. DOI: 10.1021/jp052197t

[32] Song B, Cuniberti G, Sanvito S, *et al*. Nucleobase adsorbed at graphene devices: Enhance bio-sensor ics. Appl Phys Lett, 2012, **100**: 063101. DOI: 10.1063/1.3681579

[33] Park S M and Lee H J. Recent advances in electrochemical studies of π-conjugated polymers. B Korean Chem Soc, 2005, **26**: 697–706.

[34] Mecozzi S, West A P and Dougherty D A. Cation-pi interactions in aromatics of biological and medicinal interest: electrostatic potential surfaces as a useful qualitative guide. P Natl Acad Sci USA, 1996, **93**: 10566–10571. DOI: 10.1073/pnas.93.20.10566

[35] Wouters J. Cation-π (Na$^+$-Trp) interactions in the crystal structure of tetragonal lysozyme. Protein Sci, 1998, **7**: 2472–2475. DOI: 10.1002/pro.5560071127

[36] Gallivan J P and Dougherty D A. Cation-π interactions in structural biology. P Natl Acad Sci, 1999, **96**: 9459–9464. DOI: 10.1073/pnas.96.17.9459

[37] Meyer E A, Castellano R K and Diederich F. Interactions with aromatic rings in chemical and biological recognition. Angew Chem Int Edit, 2003, **42**: 1210–1250. DOI: 10.1002/anie.200390319

[38] Hunter C A and Sanders J K M. The nature of π-π interactions. J Am Chem Soc, 1990, **112**: 5525–5534. DOI: 10.1021/ja00170a016

[39] Janiak C. A critical account on π-π stacking in metal complexes with aromatic nitrogen-containing ligands. J Chem Soc, Dalton Trans, 2000, 3885–3896. DOI: 10.1039/B003010O

[40] Meyer E A, Castellano R K and Diederish F. Interactions with aromatic rings in chemical and biological recognition. Angew Chem Int Edit, 2003, **42**: 4120. DOI: 10.1002/anie.200390319

[41] Swaddle T W, Rosenqvist J, Yu P, *et al*. Kinetic evidence for five–coordination in AlOH(aq)$^{2+}$ ion. Science, 2005, **308**: 1450–1453. DOI: 10.1126/science.1110231

[42] Kitagawa T, Ozaki Y and Kyogoku Y. Resonance Raman studies on the ligand-iron interactions in hemoproteins and metalloporphyrins. Adv Biophys, 1978, **11**: 153–196.

[43] Gallin J I and Kirkpatr C H. Chemotactic activity in dialyzable transfer factor. P Nat Acad Sci USA, 1974, **71**: 498–502. DOI: 10.1073/pnas.71.2.498

[44] Tsuzuki S, Honda K, Uchimaru T, *et al*. Origin of attraction and directionality of the π-π interaction: model chemistry calculations of benzene dimer interaction. J Am Chem Soc, 2002, **124**: 104–112. DOI: 10.1021/ja0105212

[45] Yang J W, Chen X R and Song B. Interaction of graphene-on-Al(111) composite with D-glucopyranose and its application in biodetection. J Phys Chem C, 2013, **117**: 8475–8480. DOI: 10.1021/jp311959g